



Secondary Immunization Generates Clonally Related Antigen-Specific Plasma Cells and Memory B Cells

This information is current as of August 4, 2022.

Daniela Frölich, Claudia Giesecke, Henrik E. Mei, Karin Reiter, Capucine Daridon, Peter E. Lipsky and Thomas Dörner

J Immunol 2010; 185:3103-3110; Prepublished online 6 August 2010;
doi: 10.4049/jimmunol.1000911
<http://www.jimmunol.org/content/185/5/3103>

References This article **cites 43 articles**, 21 of which you can access for free at:
<http://www.jimmunol.org/content/185/5/3103.full#ref-list-1>

Why *The JI*? [Submit online.](#)

- **Rapid Reviews! 30 days*** from submission to initial decision
- **No Triage!** Every submission reviewed by practicing scientists
- **Fast Publication!** 4 weeks from acceptance to publication

**average*

Subscription Information about subscribing to *The Journal of Immunology* is online at:
<http://jimmunol.org/subscription>

Permissions Submit copyright permission requests at:
<http://www.aai.org/About/Publications/JI/copyright.html>

Email Alerts Receive free email-alerts when new articles cite this article. Sign up at:
<http://jimmunol.org/alerts>

Errata An erratum has been published regarding this article. Please see [next page](#)
or:
</content/192/1/535.full.pdf>

Secondary Immunization Generates Clonally Related Antigen-Specific Plasma Cells and Memory B Cells

Daniela Frölich,^{*,†,1} Claudia Giesecke,^{*,†,1} Henrik E. Mei,^{*,†} Karin Reiter,^{*,†} Capucine Daridon,^{*,†} Peter E. Lipsky,[‡] and Thomas Dörner^{*,†}

Rechallenge with T cell-dependent Ags induces memory B cells to re-enter germinal centers (GCs) and undergo further expansion and differentiation into plasma cells (PCs) and secondary memory B cells. It is currently not known whether the expanded population of memory B cells and PCs generated in secondary GCs are clonally related, nor has the extent of proliferation and somatic hypermutation of their precursors been delineated. In this study, after secondary tetanus toxoid (TT) immunization, TT-specific PCs increased 17- to 80-fold on days 6–7, whereas TT-specific memory B cells peaked (delayed) on day 14 with a 2- to 22-fold increase. Molecular analyses of V_HDJ_H rearrangements of individual cells revealed no major differences of gene usage and CDR3 length between TT-specific PCs and memory B cells, and both contained extensive evidence of somatic hypermutation with a pattern consistent with GC reactions. This analysis identified clonally related TT-specific memory B cells and PCs. Within clusters of clonally related cells, sequences shared a number of mutations but also could contain additional base pair changes. The data indicate that although following secondary immunization PCs can derive from memory B cells without further somatic hypermutation, in some circumstances, likely within GC reactions, asymmetric mutation can occur. These results suggest that after the fate decision to differentiate into secondary memory B cells or PCs, some committed precursors continue to proliferate and mutate their V_H genes. *The Journal of Immunology*, 2010, 185: 3103–3110.

Serological memory plays a pivotal role in systemic protection of the host during re-exposure to hazardous pathogens and toxins. Vaccination strategies aim to stimulate this aspect of immunologic memory. The goals of vaccination are to generate Ag-specific memory B cells capable of responding to the immunizing Ag more quickly and robustly and plasma cells (PCs) secreting Abs specific for the immunizing Ag.

Primary Ag challenge leads to activation of naive B cells and subsequently generation of memory B cells expressing BCRs of increased avidity and PCs secreting high-avidity Abs. A very heterogeneous repertoire of naive B cells expressing primary BCRs is generated during B cell development by random rearrangement of V, D, and J segments of both H and L chains (1–4). Activation by T cell-dependent Ags can result in extrafollicular PC generation and formation of germinal centers (GCs). Within GCs, B cells undergo clonal expansion, somatic hypermutation, and selection as well as class switch recombination (5). These processes yield memory B cells with high-avidity BCRs and PCs secreting specific high-avidity Abs and ensure serological and reactive memory

to protect the host during secondary challenge with potentially injurious foreign materials.

Upon rechallenge with T cell-dependent Ags, memory B cells can re-enter GCs and undergo further expansion and differentiation into PCs secreting high-avidity Abs, usually of the IgG or IgA H chain isotype, and secondary memory B cells with highly mutated Ig V_H gene rearrangements. Whether the expanded population of memory B cells and PCs generated in secondary GCs are clonally related and the extent of proliferation of their precursors are currently not known.

The current study was, therefore, undertaken to address whether clonally related PCs and memory B cells emerge after antigenic rechallenge. The approach involved the simultaneous analysis of tetanus toxoid (TT)-specific PCs and memory B cells after secondary TT immunization in healthy individuals. This approach permitted the delineation of the timing of the generation of Ag-specific PCs and memory B cells. After single-cell sorting of both cell types and detailed molecular characterization of the rearranged V_HDJ_HCα/γ/μ genes, clonal relationships of PCs and memory B cells were clearly identified. Moreover, detailed analysis of somatic hypermutation of IgV_H genes of clonally related cells indicated that in some circumstances there was a remarkable degree of divergent base pair changes consistent with extensive proliferation and mutation after commitment to PC and secondary memory B cell differentiation. In other examples, memory B cells and PCs shared the same IgV_H gene rearrangements and no additional mutations, consistent with immediate PC differentiation from memory B cells without activation of somatic hypermutation.

Materials and Methods

Immunization

Six healthy Caucasian individuals (five female, one male) with a mean age of 28 y (25–33 y) received a booster immunization against TT/diphtheria toxoid (20 I.E. TT and 2 I.E. diphtheria toxoid; Sanofi Pasteur MSD, Leimen, Germany) after informed consent had been obtained from the

*Department of Medicine, Rheumatology, and Clinical Immunology, Charité University Medicine Berlin; †Deutsches Rheumaforschungszentrum Berlin, Berlin, Germany; and ‡National Institute of Arthritis and Musculoskeletal and Skin Diseases, National Institutes of Health, Bethesda, MD 20892

¹D.F. and C.G. contributed equally to this work.

Received for publication March 22, 2010. Accepted for publication June 23, 2010.

This work was supported by Deutsche Forschungsgemeinschaft Projects Do491/7-1, 2 and DO 491/5-4 and Sonderforschungsbereich 650 Project TP16.

Address correspondence and reprint requests to Prof. Thomas Dörner, Department of Medicine, Rheumatology, and Clinical Immunology, Charité University Medicine Berlin, Charitéplatz 1, Berlin 10117, Germany. E-mail address: thomas.doerner@charite.de

Abbreviations used in this paper: FR, framework; GC, germinal center; PC, plasma cell; R, replacement; rTT.C, recombinant tetanus toxoid C fragment; S, silent; TT, tetanus toxoid.

Copyright © 2010 by The American Association of Immunologists, Inc. 0022-1767/10/\$16.00

individual patients and after approval by the local ethics committee of the Charité University Medicine.

Cell preparation and staining

Peripheral blood was collected before and at various time points after immunization, and PBMCs were prepared by density gradient centrifugation using Ficoll-Paque Plus (GE Healthcare Bio-Science AB, Uppsala, Sweden) as reported previously (6). For single-cell sorting, B cells were enriched using a RosetteSep B cell enrichment kit according to the manufacturer's instructions (StemCell Technologies, Vancouver, British Columbia, Canada).

For cytometric analyses, PBMCs were incubated at 4°C for 10 min with the following fluorochrome-labeled anti-human mAbs in PBS/0.2% BSA: anti-CD19-PerCP (SJ25C1; BD Biosciences, San Jose, CA), anti-CD27-Cy5 (clone 2E4; a kind gift from René van Lier, Academic Medical Center, University of Amsterdam, Amsterdam, The Netherlands), anti-CD3-FITC (clone UCHT-1; Deutsches Rheumaforschungszentrum, Berlin, Germany), anti-CD14-FITC (clone TM1; Deutsches Rheumaforschungszentrum), TT-specific B cells were identified by binding to PE-labeled TT, and the specificity of staining was confirmed by blocking using unconjugated TT (7).

For single-cell sorting, PBMCs were stained as described above using anti-CD3-Pacific blue, anti-CD14-Pacific blue (clone M5E2; BD Biosciences), anti-CD19-PECy7, anti-CD27-Cy5, anti-CD20-PerCP (clone L27; BD Biosciences) and digoxigenated recombinant C-fragment of tetanus toxin (rTT.C; Hoffmann-La Roche, Indianapolis, IN, conjugated to digoxigenin, Boehringer, Mannheim, Germany). This approach was employed because it consistently gave better separation of Ag-specific and nonspecific cells. After being washed with PBS/BSA, cells were incubated with anti-digoxigenin-FITC (Boehringer and Deutsches Rheumaforschungszentrum) at 4°C for 10 min. DAPI (Molecular Probes, Eugene, OR) was added immediately before cytometric analysis or cell sorting to exclude dead cells.

Cytometric analyses, phenotyping, and cell enumeration

Cytometric analyses of TT-specific cells were performed for three donors (#1, #2, and #3) on days 0, 2, 5, 6, 7, 8, 9, 12, 14, and 20 and additionally for donor #2 on day 41 after vaccination. Flow cytometric data were analyzed using FlowJo software (Tree Star, Ashland, OR). Peripheral blood B cells were quantified as described previously using the TruCount system (BD Biosciences) (8). Absolute numbers of TT-specific PCs (CD19⁺, CD27⁺⁺, CD3⁻, CD14⁻) and memory B cells (CD19⁺, CD27⁺, CD3⁻, CD14⁻) were then calculated.

Cell sorting and cDNA synthesis

Seven days after immunization single CD19⁺, CD27⁺⁺, CD20⁻, CD3⁻, CD14⁻, rTT.C-specific PCs and 9 d after immunization single CD19⁺, CD27⁺, CD20⁺, CD3⁻, CD14⁻, rTT.C-specific memory B cells of three donors (#4, #5, and #6) were sorted into 96-well plates using a FACSAria (BD Biosciences). Each well contained a reaction mix as described elsewhere (9), and first strand cDNA was generated at 50°C for 60 min.

Nested PCR

Nested isotype-specific (IgA/IgG/IgM) PCRs were performed to amplify the rearranged V_HDJ_HC_α/γ/μ cDNAs, respectively. For external PCR, 5 μl of the amplified cDNA was used as template and a PCR mix as previously described (10). The cycle program consisted of 7 min at 95°C, 1 min at 50°C, 90 s at 72°C, followed by 50 cycles of 1 min at 94°C, 30 s at 50°C, 90 s at 72°C, and to finish 1 min at 94°C, 30 s at 50°C, 10 min 72°C. The internal PCR was performed in an identical manner, except for the annealing temperature, which was set to 58°C, and 5 μl of the reaction products from the external PCR was used as template.

The sequences of the isotype-specific 3' primers are shown in Table I. For the family-specific external and internal 5' primers, oligonucleotides were employed as described previously (11, 12).

Sequence analysis

PCR products were separated by agarose gel electrophoresis, visualized with ethidium bromide by exposure to UV light, cut out and purified using a QIAquick gel extraction kit (Qiagen, Hilden, Germany) according to the manufacturer's instructions. Products were sequenced at Eurofins MWG Operon (Martinsried, Germany). Sequences were analyzed using the Chromas 2.33 sequence viewer (Chromas Technelysim, Helensvale, Australia), the basic local alignment search tool algorithm of the National Center for Biotechnology Information (www.ncbi.nlm.nih.gov), and the software JOINSOLVER (<http://joinsolver.niams.nih.gov>) (13). Sequences containing a stop codon or an out-of-frame rearrangement were considered as nonproductive and excluded from the analysis. Genomatix (www.genomatix.de/cgi-bin/dialign/dialign.pl) (14) was used for alignments and homology analyses of the sequences. Phylograms were created using Phylogeny.fr (www.phylogeny.fr) (15).

Statistical analysis

Prism, version 4, for Windows (GraphPad Software, San Diego, CA; www.graphpad.com) was used for statistical analyses. To determine significant differences in distributions of gene usage, replacement (R) to silent (S) mutations ratio, and mutational hotspots between rTT.C-specific PCs and memory B cells, the χ^2 test was used. Additionally, Mann-Whitney *U* tests were performed to analyze CDR3 lengths and mutational rates. Dependence of mutation frequency on V_H family was tested using one-way ANOVA. The *p* values ≤ 0.05 were considered to reflect a significant difference.

Statistical calculation of repertoire sizes

The theoretical repertoire size and the potential number of Ag-specific clones were calculated according to Behlke et al. (16) based on the obtained data. Therefore, the probability $P(d)$ of observing d different gene rearrangements (i.e., distinct sequences) among a total number of r examined sequences for a fixed number n of different gene rearrangements is

$$P(d) = S(r, d) \binom{n}{d} d! n^{-r}, \quad (1)$$

where $S(r, d)$ are Stirling's numbers of the second kind. A 95% one-sided confidence of the estimates was calculated by determining the smallest value of n for which the probability of observing d different gene rearrangements among r examined sequences was < 0.05 .

Results

Different kinetics of TT-specific PCs and memory B cells after tetanus booster

Direct labeling of PBMCs with PE-conjugated TT was used to determine the kinetics of the appearance of TT-specific PCs and memory B cells in the blood of three healthy donors after secondary TT immunization. Simultaneous cytometric detection of TT-specific PCs (CD19⁺, CD27⁺⁺) and memory B cells (CD19⁺, CD27⁺) was performed (Fig. 1A, donor #2), and their absolute cell numbers were calculated (Fig. 1B). Specificity of the staining was confirmed by blocking using unconjugated TT as reported previously (7).

Before TT vaccination (day 0), a mean of 87 TT-specific PCs per milliliter (range 31–168) and a mean of 73 memory B cells per milliliter (range 31–122) were detected. After secondary immunization, the total number of TT-specific PCs and memory B cells increased. The kinetics of appearance of each TT-specific cell type was similar for all three donors analyzed. TT-specific PCs increased to an average of 5239 cells per milliliter (range 1037–13,493) on

Table I. Sequences of isotype-specific primers for nested PCR

External 3' primer	IgVH α (43)	5'-GGA AGA AGC CCT GGA CCA GGC-3'
	E γ	5'-AC GCC GCT GGT CAG GGC GC-3'
	E μ	5'-TCA GGA CTG ATG GGA AGC CC-3'
Internal 3' primer	IgA α 2 (43)	5'-ACC AGG CAG GCG ATG ACC AC-3'
	IgG α ^a	5'-AAG TAG TCC TTG ACC AGG CAG C-3'
	IgMin _{neu}	5'-AGG AGA CGA GGG GGA AAA GGG TTG-3'

^aIgG α and IgMin_{neu} both have been modified after Yavuz et al. (44).

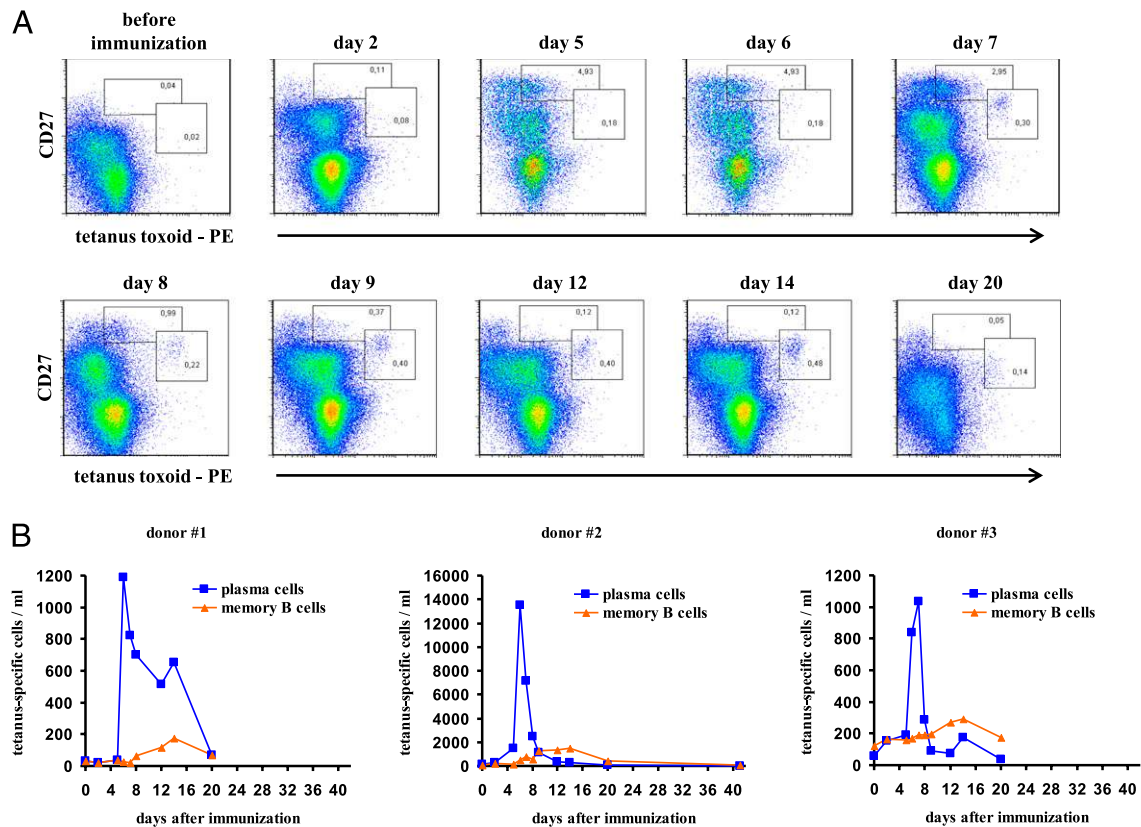


FIGURE 1. Kinetics of TT-specific PCs and memory B cells in peripheral blood. *A*, Dot plots of cytometric analysis of PE-labeled TT-specific CD19⁺, CD27⁺, CD3⁻, CD14⁻ PCs and CD19⁺, CD27⁺, CD3⁻, CD14⁻ memory B cells of donor #2. *B*, Time course of appearance of PCs and memory B cells for each donor. Blue diamonds and orange squares indicate time points of blood analyses.

days 6–7, which approximates a 17- to 80-fold increase. In contrast, TT-specific memory B cells peaked on day 14 after secondary immunization with a maximum of 651 cells per milliliter (range 175–1486), approximating a 2- to 22-fold increase. In each donor, the increase in TT-specific memory B cells appeared delayed and had a consistently lower maximum peak compared with that of TT-specific PCs (3.5- to 9-fold difference).

Molecular analyses

The reproducible time shift in the maximal appearance of TT-specific memory B cells compared with that of PCs led to the question whether they were clonally related. To determine the relationship between these cell populations, single CD19⁺, CD27⁺, CD20⁻, CD3⁻, CD14⁻, rTT.C-specific PCs and single CD19⁺, CD27⁺, CD20⁺, CD3⁻, CD14⁻, rTT.C-specific memory B cells from three donors were sorted and analyzed for rearranged V_HDJ_HCα/γ/μ genes after secondary immunization.

For donor #4, 77 productive sequences out of 96 sorted PCs (77/96) were obtained, and 1 sequence out of 10 sorted memory B cells (1/10) was obtained. For donor #5 30/34 PCs and 12/54 memory B cells and for donor #6 19/25 PCs and 7/26 memory B cells were obtained. Altogether, six nonproductive sequences were found and were not further included in the statistical analysis. Accordingly, 126 Ig V_H sequences from PCs (recovery rate 81.3%) and 20 memory B cell-derived IgV_H sequences (recovery rate 22.2%) were available for analyses.

Initially, the isotypes of the expressed Igs were determined by sequence comparison of the isotype-specific fragment with germline constant regions (basic local alignment search tool). Approximately 95% of rTT.C-specific PCs and memory B cells expressed the IgG isotype. The most commonly expressed subclass was IgG₁

(116 cells out of 126 analyzed PCs, 18 cells out of 20 analyzed memory B cells), followed by IgG₂ (5/126, 1/20), IgA₁ (2/126, 1/20), IgG₄ (2/126, 0/20), and IgM (1/126, 0/20). The subclasses IgG₃ and IgA₂ were not found among the sequences analyzed. No significant difference was found in the distribution of IgH isotypes between rTT.C-specific PCs and memory B cells.

Next, all of the sequences were analyzed with regard to their V_H and J_H gene segment usage, CDR3 length, and sequence as well as the frequency and distribution of somatic hypermutations. Clonally related sequences from each donor were found. From donor #4, 44 clonally related PC sequences out of 77 analyzed were found, whereas in donor #5 8 out of 30 and in donor #6 5 out of 19 analyzed PC sequences were found. Among the memory B cells two clonally related sequences were found (donor #6). Thus, clonally related cells with the same V_HDJ_H rearrangements and CDR3 sequences were routinely found.

Comparable usage of V_H and J_H gene segments in rTT.C-specific PCs and memory B cells

To determine the individual gene segments employed by V_HDJ_H rearrangements, the closest germline gene segments were identified using JOINSOLVER and the Kabat et al. (17) database. For this analysis, only clonally unrelated sequences were used (69 from PCs, 19 from memory B cells), whereas clonally related cells were considered in the molecular analyses as one cell (separately for each cell population). The distributions of the V_H gene segments and J_H gene segments by rTT.C-specific PC and memory B cell sequences are shown in Fig. 2. Except for V_H6 and V_H7, gene segments of all V_H and J_H families were found. V_H4 was expressed most frequently by PCs (29/69), followed by V_H3 (21/69), V_H1 (7/69), V_H2 (7/69), and V_H5 (5/69). In memory B cells, V_H3 (7/19) was

the most frequently expressed V_H family, followed by V_{H4} (5/19), V_{H1} (4/19), V_{H5} (2/19), and V_{H2} (1/19) (Fig. 2A).

Analysis of the J_H gene segment usage revealed that J_{H4} was used most frequently by PCs (29/69), followed by J_{H5} (17/69), J_{H3} (11/69), J_{H6} (10/69), and J_{H1} (2/69). In memory B cells, J_{H4} (8/19) was also used most frequently, followed by J_{H3} (5/19), J_{H5} (4/19), J_{H2} (1/19), and J_{H6} (1/19) (Fig. 2B). Of note, no significant difference was found in the distribution of V_H and J_H family usage between rTT.C-specific PCs and memory B cells.

Similar distribution of CDR3 lengths in rTT.C-specific PCs and memory B cells

CDR3 lengths (Fig. 3A) and CDR3 sequences (data not shown) critically involved in Ag recognition by epitope binding were further analyzed in detail. In rTT.C-specific PCs and memory B cells, the respective CDR3s comprised 30–69 bp, whereas maxima of occurrence were found at 30 and 45 bp in both populations.

Similar frequency and distribution of somatic hypermutations

The frequency and characteristics of somatic hypermutations in rearranged V_H gene segments were analyzed using JOINSOLVER. Mutation frequencies ranged between 0 and 18.2% (median 9.65%) in PCs and between 2.2 and 20.3% (median 9.61%) in memory B cells (Fig. 3B). Of note, the mutation frequencies were independent of the individual V_H family used (one-way ANOVA).

An important characteristic of affinity maturation in B cells is the enhanced R/S ratio of R to S mutations within the expressed V_H gene segment. In CDRs as well as framework regions (FRs), more R than S mutations were found. Some sequences lacked S mutations, especially in the CDRs, and therefore, the R/S ratio was calculated using the accumulated number of R and S mutations. The R/S ratios within CDRs were increased (3.6 in PCs and 3.7 memory B cells) compared with those in FRs (1.5 and 1.6).

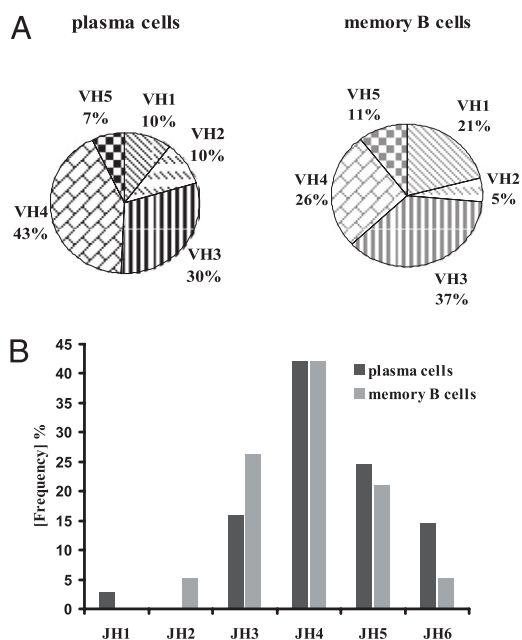


FIGURE 2. Similar distributions of V_H and J_H family usage by rTT.C-specific PCs and memory B cells of three donors after tetanus booster. *A*, Distribution of V_H family usage. *B*, Distribution of J_H family usage. PCs were collected 7 d after tetanus immunization, and memory B cells were collected 9 d after tetanus immunization. Pooled results from three donors are shown. No significant differences were observed (χ^2 test) in the V_H and J_H family usage between PCs and memory B cells.

Analysis of R/S ratios of additional accumulated mutations within trees of clonally related PCs and memory B cells (Fig. 4B, clones a, b, d, g) revealed a lower R/S ratio of 1.2 within CDRs and a ratio of 1.7 within FRs.

Of note, the mutational machinery targets mutations into specific RGYW/WRCY motifs on both DNA strands. Accordingly, 55% of the mutations found in PCs occurred within a mutation hotspot (RGYW or WRCY) (18), whereas 49% of mutations were identified within these motifs in sequences obtained from memory B cells ($p = 0.0213$, χ^2 test). Interestingly, the observed frequencies were ~ 2 -fold higher than expected (18).

Sequence alignments of PCs and memory B cells disclosed clonal relationships

To determine the relationship between rTT.C-specific PCs and memory B cells for each donor, all of the sequences (V_HDJ_H region) were aligned. In all three donors, clonally related PCs and memory B cells based on the same V_H and J_H gene segment usage and CDR3 sequence were found. The phylogram in Fig. 4A illustrates the clonal relationships for donor #6.

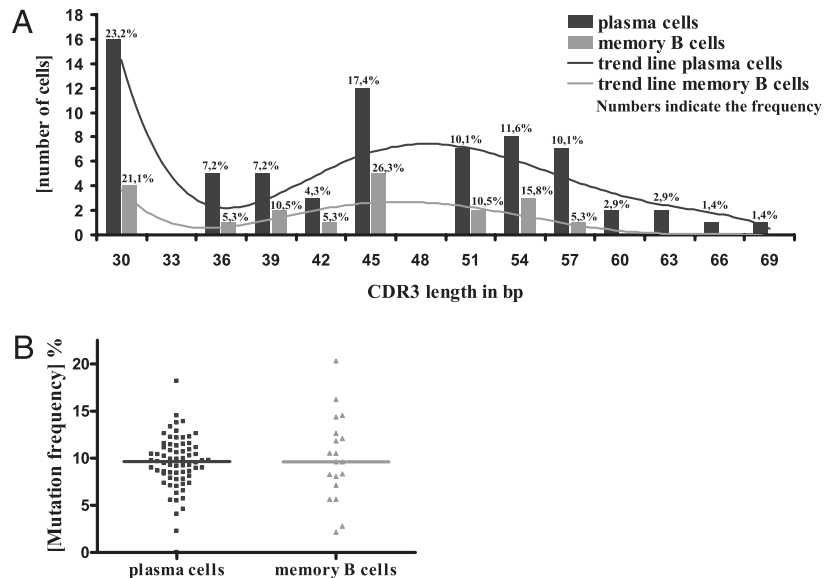
For 8 out of 20 rTT.C-specific memory B cells, clonally related PCs were found (1–3 PCs). Within a family of clonally related cells, the sequence homology ranged between 87 and 100%. In one case, two clonally related memory B cells were present (sequence homology 88%), and 21 groups of clonally related PCs (2–14 cells) were found. Within families of clonally related cells, detailed analysis of sequences revealed that these cells shared a number of mutations but often also expressed additional base pair changes (Fig. 4B). For example, one clonal tree from donor #6 (clone b) showed that clonally related PCs and memory B cells had as many as 18 and 17 different base pair changes. Similarly, clonally related memory B cells and PCs from donor #5 (clone d) had as many as 27 different mutations. In both circumstances, the differences related to the acquisition of new mutations by both rTT.C-specific memory B cells and PCs. In two clones from donor #5 (clones e and f), no additional mutations were found in memory B cells and PCs. It is notable that in these clones a large number of mutations (23 and 22) were likely to have occurred in the common precursor. Notably, no cell with the same or related sequence was found in any two of the three donors. Finally, the IgVH rearrangement sequences of clonally related memory cells and PCs were identical with those of their presumed precursor in three examples of donor #1 (clone c) and #2 (clones e and f) (Fig. 4B), whereas in all three donors continuous acquisition of mutations within memory cells and PCs was identified (clones a, b, d, and g).

Statistical analysis of repertoire sizes

As shown in the analyses described above, for each donor the number of different V_HDJ_H rearrangements (i.e., sequences) was lower than the total number of analyzed sequences. Accordingly, for donor #4, 33 unequal PC sequences out of 77 analyzed PC were obtained, for donor #5 22 out of 30, and for donor #6 14 out of 19. On the basis of this data, the theoretical statistical repertoire size specific against TT was calculated. For this calculation, it was assumed that no significant skewing of the data set by nonrandom gene segment usage occurred as described elsewhere (16).

For each donor, the statistical/theoretical rTT.C-specific repertoire size (i.e., theoretical number of all rTT.C-specific distinct rearrangements) has been calculated from the number of examined sequences and the number of different rearrangements observed. This analysis revealed a 95% one-sided confidence bound n for each donor by determining the smallest value of n for which the probability of observing at most d different sequences among r total examined sequences was < 0.05 . Thus, n is the theoretical

FIGURE 3. CDR3 lengths and mutation frequencies of rTT.C-specific PCs and memory B cells. *A*, Distribution of CDR3 length. Frequencies refer to absolute numbers of analyzed PCs and respective memory B cells. *B*, Scatter plot of mutation frequencies. The bar indicates the median. No significant differences were observed (χ^2 test, Mann-Whitney *U* test) between PCs and memory B cells in both parameters. Clonally related cells were counted only once.



statistical calculated quantity of different clones within one individual to ensure (with a 95% confidence) the empirical found numbers of observed distinct sequences among all of the examined sequences. As a result and by application of this equation, the statistical estimated repertoire size n for donor #4 was 44, for donor #5 79, and for donor #6 64, which appeared to be remarkably similar between the different individuals.

Discussion

The differentiation pathway of memory B cells after secondary immunization is not well understood. For the first time, to the best of our knowledge, molecular characteristics of both tetanus-specific human PCs and memory B cells after secondary immunization have been analyzed within the same donors. PCs and memory B cells having identical CDR3 sequences were identified in the blood, clearly indicating that precursors of secondary memory B cells and PCs are clonally related. The observation that some of the clones have divergent patterns of somatic hypermutation suggests that memory B cell precursors of both secondary memory B cells and PCs mainly continue to divide and undergo further rounds of somatic hypermutation after the decision to differentiate into one or the other has been completed. Although this represents a new alternative, other clones of memory B cells and PCs carrying the very same IgVH gene sequences with no additional mutations were also found, consistent with the conclusion that they were induced simultaneously out of their precursor cells without activation of somatic hypermutation.

Kinetics

To investigate the kinetics and magnitude of the human PC and memory B cell response after TT booster, absolute numbers of these two cell populations were determined in the peripheral blood. The maximum of TT-specific PC and memory B cell numbers were observed on day 7 and day 14, respectively, after secondary immunization. This is in concordance with previous studies monitoring immune responses after TT (7, 19) or influenza immunization (20, 21). In these studies, peaks of Ag-specific PCs and memory B cells could be observed on days 6–8 and 14–28, respectively. Furthermore, the smaller absolute number of memory B cells compared with PCs (3.5- to 9-fold) is consistent with results of a previous study (10-fold) (7). At the peak of the response, TT-specific PCs represented ~13% of the total CD19⁺/CD27⁺⁺ population (data not shown). Moreover, these cells were both Ki-67⁺ and

HLA-DR^{high}, marking them as plasmablasts recently generated from proliferating precursors (7, 20). The distinct kinetics of rapid detection of increased numbers of Ag-specific PCs and delayed occurrence of increases in memory B cell numbers suggest either a difference in the timing of their generation or a dichotomy in the expression or function of adhesion molecules, chemokine receptors, or other molecules involved in their migration and/or tissue localization. In this regard, in mice and humans, it has been shown that PCs lack CXCR5 expression or express it at marginal levels (22, 23). CXCR5 is important for follicular localization (24) and essential for homing to secondary lymphoid tissues (25). Thus, PCs may have decreased migratory capacities toward the follicles in lymph nodes or spleen. Memory B cells still express CXCR5, and their egress from GCs apparently is differently regulated (24).

Molecular analyses

To determine the relationship between rTT.C-specific PCs and memory B cells, comprehensive molecular analyses of single sorted cells were performed. The analyses of rTT.C-specific PCs revealed that ~95% of these cells expressed the IgG H chain isotype, suggesting their origin from T cell-dependent memory B cell activation. This is in line with previous reports in which >90% of tetanus-fragment C⁺ PCs produced IgG (19). In addition, influenza-vaccine-specific Ab-secreting cells were reported to secrete mainly IgG (20). In contrast, most of the human peripheral blood PCs in the steady state expressed intracellular IgA (8), likely being induced in the gut instructed under the influence of the IgA switch factors, TGF- β and a proliferation-inducing ligand (26, 27).

The V_H and J_H family usage of rTT.C-specific PCs showed no statistical difference among the three analyzed donors. This is in contrast to a previous study that reported an extensive diversity in the TT-specific repertoires from different subjects (28). However, when the rTT.C-specific V_H and J_H family usage was compared with a previously reported unselected repertoire from peripheral IgM⁺ B cells (29), a significant difference ($p < 0.0001$, χ^2 test) was found, presumably as a result of selection, suggesting the possibility that elements of both V_H and J_H segments might contribute to Ag specificity.

Notably, rTT.C-specific PCs had highly mutated V_H gene rearrangements (a mean of ~20.5 mutations), comparable to other reports of the highly mutated nature of the Ig V_H genes of Ag-specific PCs

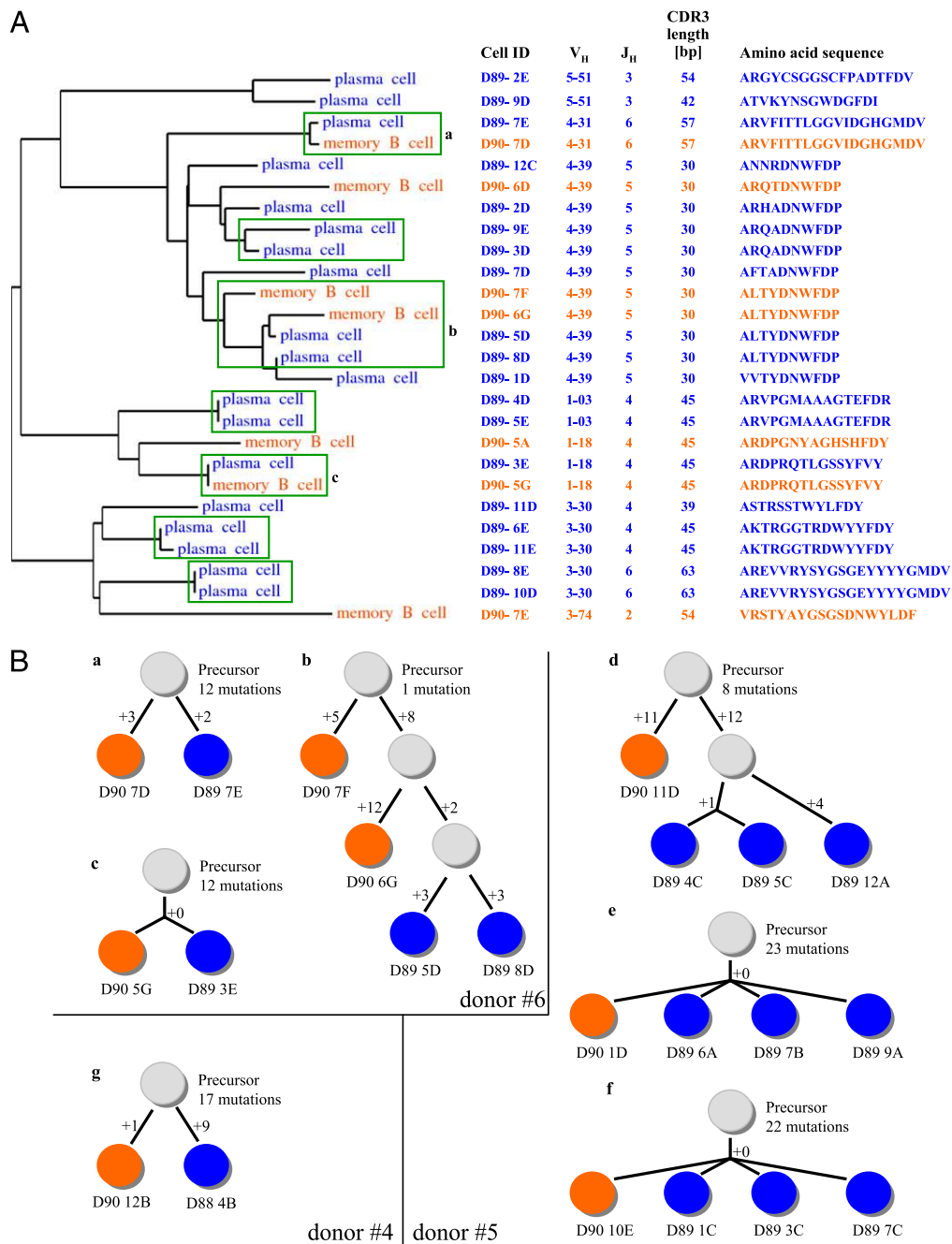


FIGURE 4. Relationship between rTT.C-specific PCs and memory B cells. *A*, Phylogram of the relationship between rTT.C-specific PCs (blue) and memory B cells (orange) of one donor (donor #6). Clonally related cells (same V_HDJ_H recombination and same CDR3 nucleotide sequence [data not shown]) are boxed by a green rectangle. Clones a, b, and c are clusters of clonally related cells containing both PCs and memory B cells, which are further analyzed in *B*. The table gives further specifications for each cell including the amino acid sequence of each respective CDR3. The phylogram was created using Phylogeny.fr (accessed July 20, 2009). *B*, Schematic mutation trees showing memory B cells with their clonally related PCs (donors #4, #5, and #6). Blue circles indicate found PC sequences, and orange circles found memory B cell sequences. Gray circles denote hypothetical intermediate sequences (cells) that are not found but have mutations that are shared by all subsequent sequences (cells). Numbers in branches indicate the numbers of mutations to the next node. Clones a, b, d, and g were further analyzed for their additional mutations (i.e., additional accumulated mutations not yet present in the predicted precursors).

(mean of 18–19 mutations) (20). On the basis of the very high frequency of mutations and the development of increased numbers of circulating PCs 6–7 d after secondary immunization, it can be assumed that pre-existing memory B cells and not naive B cells were the major precursor of the PCs analyzed. On the basis of the previous estimate of the mutation rate as one mutation per 1000 bp per cell division (30), it would require more than 90 cell divisions to result in a mean of 20 mutations per 210 bp of analyzed V_H region. Such

a scenario appears to be unlikely within a 6–7 d period because the minimal cell cycle length of GC B cells ranges between 6 (31) and 12 h (32). Consistent with this, a previous study showed that after primary immunization of mice Ag-specific GC-derived B cells in the peripheral blood 7 d later exhibited a mean mutation frequency of 0.1%. By 10 d, this had increased to 1.2%, and even on day 28 after primary immunization the mutation frequency was <5% (33). These results are, therefore, most consistent with the conclusion

that the rTT.C-specific PCs are the progeny of previously mutated memory B cells.

Additionally, the data also suggest that the immediate precursors of these memory B cell-derived PCs retain the capacity to undergo further somatic hypermutation. Whether the capacity to undergo additional somatic hypermutation contributes to further avidity maturation is currently unknown. The presence of additional mutations implies that PC precursors may continue to mutate and proliferate. The finding that the PCs induced by secondary immunization with TT are Ki-67⁺ is consistent with this conclusion (8). Finally, the observation that both rTT.C-specific PCs and memory B cells have acquired unique mutations indicates that each committed precursor retained the capacity to mutate and proliferate after the decision to become either effector cell type had been made. Of interest, the finding that clonally related rTT.C-specific memory B cells and PCs have different mutational patterns suggests that they may not have the exact same Ag binding characteristics.

High R/S ratios were demonstrated in the memory B cell and PC V_H sequences and indicate a preference of R mutations within the CDRs. This is considered to be an indication of affinity maturation and antigenic selection (19), although the general tendency of the mutational machinery to introduce R mutations in the CDRs of V_H segments makes this contention uncertain (34). Intriguingly, a 3-fold reduced R/S ratio (1.2) was detected within CDRs compared with the R/S ratio within CDRs (~3.6) for all mutations when the R/S ratio of additional mutations accumulated uniquely within clonally related PCs and memory B cells was analyzed. This is consistent with the hypothesis that the cells analyzed in this study were derived from already existent memory B cells with high-affinity BCRs. Additional activity of the mutation machinery is unlikely to increase avidity greatly but also carries the risk of inducing nonsense mutations leading to a loss of the B cell from the repertoire (34). The accumulated mutations within RGYW/WRCY motifs were much greater than expected from random chance and are consistent with T cell-dependent and CD40- and CD154-mediated responses, because targeting of mutations into RGYW/WRCY motifs is deficient in CD154-deficient subjects (35). Taken together, the mutational data imply that the base pair changes found in both secondary memory B cells and PCs arose from T cell-dependent responses and perhaps reflect avidity maturation.

rTT.C-specific memory B cells did not differ significantly from the rTT.C-specific PCs regarding their V_H and J_H family usage, CDR3 lengths, mutation frequencies, and R/S ratios. Thus, most of the rTT.C-specific PCs and memory B cells may have passed through a similar microenvironment in the GC. Moreover, the evidence indicates that PCs and secondary memory B cells can arise from the same memory B cell precursor. In support of this conclusion, a phylogram identified clonally related PCs and memory B cells within all three donors. Because of the random rearrangement of gene segments (V_H, D, and J_H) and the activity of exonuclease and terminal deoxynucleotidyl transferase activity editing the junctional regions of the segments, a theoretically infinite number of possible BCR sequences can be produced. Therefore, the probability of finding independently developed B cells with identical BCR sequences is highly unlikely. Consistent with this conclusion, no sequences with the same V_HDJ_H recombination were found among the three individual donors. However, the study identified clonally related rTT.C-specific PCs and memory B cells within each donor, suggesting that these cells descended from a common precursor even though they appeared in the peripheral blood at different time points. Because the clonally related memory B cells and PCs shared a number of common mutations, it is highly likely that both originated from previously mutated memory B cell precursors. In this context, the

theoretical rTT.C-specific repertoire size was estimated. As a result, the calculated rTT.C-specific repertoire sizes ranged between 44 and 79 different clones among the three donors. This is comparable to a previous study where the TT-specific repertoire was estimated to be on the order of 100 distinct B cell clones using different detection methods (28). However, the actual repertoire sizes might be slightly larger than estimated by the statistical calculation, because rTT.C contains only ~50% of the TT epitopes.

As discussed above, the timing of the appearance of secondary memory B cells and PCs in the blood makes their origin from naive B cells unlikely. Although some examples of clonally related cells with identical sequences support the classical view that memory B cells and PCs are induced from memory B cells without additional somatic hypermutation, it is important to emphasize that in other examples both rTT.C-specific memory B cell and PC clones expressed independent mutations in all three donors, suggesting the possibility that each cell maintained the capacity to proliferate and mutate after a fate decision had been made to mature into either of the effector B cell types. Finally, it should be noted that it is possible that the commitment to differentiate into a secondary memory B cell or a PC did not occur in response to the secondary immunization but rather had occurred during a previous antigenic exposure. Although the current data do not address that possibility, it is important to realize that in either scenario memory B cell precursors of secondary memory B cells and PCs would be required to proliferate and mutate after a fate decision concerning further differentiation had been made.

Accordingly, an alternative hypothetical model compared with that of Liu et al. (36) can be proposed (Fig. 5) in which resting memory B cells that divide rarely in the context of self renewing (37–39) are induced to undergo rapid clonal expansion in response to Ag activation. Some of these cells rapidly differentiate into PCs and memory B cells with no further somatic hypermutation. Others have the capacity to enter a GC to undergo further proliferation and somatic hypermutation. At some point during the GC reaction, a fate decision is made concerning subsequent differentiation into

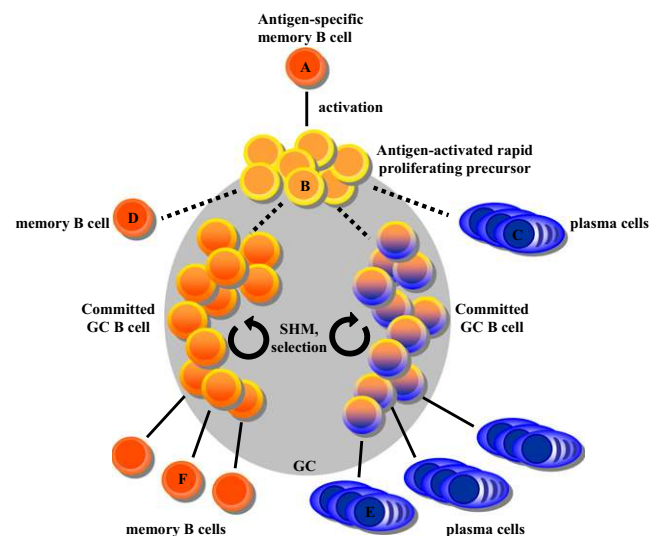


FIGURE 5. Schematic model for the generation of Ag-specific PCs and memory B cells after booster. Ag-specific memory B cells (A), generated during previous Ag challenges, become rapid proliferating cells (B) upon activation. These can either directly undergo differentiation into PCs (C) or secondary memory B cells (D) sharing identical sequences or enter into GCs. Here, after the fate decision between secondary memory B cells and PCs, committed GC B cells undergo further proliferation and somatic hypermutation. Eventually high-affinity PCs (E) and secondary memory B cells (F) differing in their mutational patterns are released from the GC.

secondary memory B cells or PCs. After this decision, the committed precursors continue to proliferate and mutate their Ig V_H genes. Expression of master regulatory genes, such as BLIMP-1, determines this decision, probably influenced by both Ag avidity and density, and the impact of T cells helps, including CD40 and IL-21 signaling (40–42).

Acknowledgments

We thank T. Kaiser and K. Raba for excellent assistance with cell sorting.

Disclosures

The authors have no financial conflicts of interest.

References

- Ollila, J., and M. Vihinen. 2005. B cells. *Int. J. Biochem. Cell Biol.* 37: 518–523.
- Rajewsky, K. 1996. Clonal selection and learning in the antibody system. *Nature* 381: 751–758.
- Grawunder, U., R. B. West, and M. R. Lieber. 1998. Antigen receptor gene rearrangement. *Curr. Opin. Immunol.* 10: 172–180.
- Jung, D., and F. W. Alt. 2004. Unraveling V(D)J recombination; insights into gene regulation. *Cell* 116: 299–311.
- Klein, U., and R. Dalla-Favera. 2008. Germinal centres: role in B-cell physiology and malignancy. *Nat. Rev. Immunol.* 8: 22–33.
- Odendahl, M., A. Jacobi, A. Hansen, E. Feist, F. Hiepe, G. R. Burmester, P. E. Lipsky, A. Radbruch, and T. Dörner. 2000. Disturbed peripheral B lymphocyte homeostasis in systemic lupus erythematosus. *J. Immunol.* 165: 5970–5979.
- Odendahl, M., H. Mei, B. F. Hoyer, A. M. Jacobi, A. Hansen, G. Muehlinghaus, C. Berek, F. Hiepe, R. Manz, A. Radbruch, and T. Dörner. 2005. Generation of migratory antigen-specific plasma blasts and mobilization of resident plasma cells in a secondary immune response. *Blood* 105: 1614–1621.
- Mei, H. E., T. Yoshida, W. Sime, F. Hiepe, K. Thiele, R. A. Manz, A. Radbruch, and T. Dörner. 2009. Blood-borne human plasma cells in steady state are derived from mucosal immune responses. *Blood* 113: 2461–2469.
- Hansen, A., K. Reiter, T. Dörner, and A. Pruss. 2005. Cryopreserved human B cells as an alternative source for single cell mRNA analysis. *Cell Tissue Bank* 6: 299–308.
- Foster, S. J., H. P. Brezinschek, R. I. Brezinschek, and P. E. Lipsky. 1997. Molecular mechanisms and selective influences that shape the kappa gene repertoire of IgM+ B cells. *J. Clin. Invest.* 99: 1614–1627.
- Campbell, M. J., A. D. Zelenetz, S. Levy, and R. Levy. 1992. Use of family specific leader region primers for PCR amplification of the human heavy chain variable region gene repertoire. *Mol. Immunol.* 29: 193–203.
- Marks, J. D., M. Tristem, A. Karpas, and G. Winter. 1991. Oligonucleotide primers for polymerase chain reaction amplification of human immunoglobulin variable genes and design of family-specific oligonucleotide probes. *Eur. J. Immunol.* 21: 985–991.
- Souto-Carneiro, M. M., N. S. Longo, D. E. Russ, H. W. Sun, and P. E. Lipsky. 2004. Characterization of the human Ig heavy chain antigen binding complementarity determining region 3 using a newly developed software algorithm, JOINSOLVER. *J. Immunol.* 172: 6790–6802.
- Morgenstern, B., A. Dress, and T. Werner. 1996. Multiple DNA and protein sequence alignment based on segment-to-segment comparison. *Proc. Natl. Acad. Sci. USA* 93: 12098–12103.
- Dereeper, A., V. Guignon, G. Blanc, S. Audic, S. Buffet, F. Chevenet, J. F. Dufayard, S. Guindon, V. Lefort, M. Lescot, et al. 2008. Phylogeny.fr: robust phylogenetic analysis for the non-specialist. *Nucleic Acids Res.* 36(Web Server issue): W465–W469.
- Behlke, M. A., D. G. Spinella, H. S. Chou, W. Sha, D. L. Hartl, and D. Y. Loh. 1985. T-cell receptor beta-chain expression: dependence on relatively few variable region genes. *Science* 229: 566–570.
- Kabat, E. A., T. T. Wu, H. M. Perry, K. S. Gottesman, and C. Foeller. 1991. *Sequences of Proteins of Immunological Interest*, 5th Ed. Public Health Service, National Institutes of Health, Washington, DC.
- Rogozin, I. B., and N. A. Kolchanov. 1992. Somatic hypermutagenesis in immunoglobulin genes. II. Influence of neighbouring base sequences on mutagenesis. *Biochim. Biophys. Acta* 1171: 11–18.
- González-García, I., B. Rodríguez-Bayona, F. Mora-López, A. Campos-Caro, and J. A. Brieve. 2008. Increased survival is a selective feature of human circulating antigen-induced plasma cells synthesizing high-affinity antibodies. *Blood* 111: 741–749.
- Wrammert, J., K. Smith, J. Miller, W. A. Langley, K. Kokko, C. Larsen, N. Y. Zheng, I. Mays, L. Garman, C. Helms, et al. 2008. Rapid cloning of high-affinity human monoclonal antibodies against influenza virus. *Nature* 453: 667–671.
- Pinna, D., D. Corti, D. Jarrossay, F. Sallusto, and A. Lanzavecchia. 2009. Clonal dissection of the human memory B-cell repertoire following infection and vaccination. *Eur. J. Immunol.* 39: 1260–1270.
- Medina, F., C. Segundo, A. Campos-Caro, I. González-García, and J. A. Brieve. 2002. The heterogeneity shown by human plasma cells from tonsil, blood, and bone marrow reveals graded stages of increasing maturity, but local profiles of adhesion molecule expression. *Blood* 99: 2154–2161.
- Nakayama, T., K. Hieshima, D. Izawa, Y. Tatsumi, A. Kanamaru, and O. Yoshie. 2003. Cutting edge: profile of chemokine receptor expression on human plasma cells accounts for their efficient recruitment to target tissues. *J. Immunol.* 170: 1136–1140.
- Wehrli, N., D. F. Legler, D. Finke, K. M. Toellner, P. Loetscher, M. Baggiolini, I. C. MacLennan, and H. Acha-Orbea. 2001. Changing responsiveness to chemokines allows medullary plasmablasts to leave lymph nodes. *Eur. J. Immunol.* 31: 609–616.
- Förster, R., A. E. Mattis, E. Kremmer, E. Wolf, G. Brem, and M. Lipp. 1996. A putative chemokine receptor, BLR1, directs B cell migration to defined lymphoid organs and specific anatomic compartments of the spleen. *Cell* 87: 1037–1047.
- Stavnezer, J., and J. Kang. 2009. The surprising discovery that TGF beta specifically induces the IgA class switch. *J. Immunol.* 182: 5–7.
- He, B., W. Xu, P. A. Santini, A. D. Polydorides, A. Chiu, J. Estrella, M. Shan, A. Chadburn, V. Villanacci, A. Plebani, et al. 2007. Intestinal bacteria trigger T cell-independent immunoglobulin A(2) class switching by inducing epithelial-cell secretion of the cytokine APRIL. *Immunity* 26: 812–826.
- Poulsen, T. R., P. J. Meijer, A. Jensen, L. S. Nielsen, and P. S. Andersen. 2007. Kinetic, affinity, and diversity limits of human polyclonal antibody responses against tetanus toxoid. *J. Immunol.* 179: 3841–3850.
- Brezinschek, H. P., S. J. Foster, R. I. Brezinschek, T. Dörner, R. Domiati-Saad, and P. E. Lipsky. 1997. Analysis of the human VH gene repertoire. Differential effects of selection and somatic hypermutation on human peripheral CD5 (+)/IgM+ and CD5(-)/IgM+ B cells. *J. Clin. Invest.* 99: 2488–2501.
- McKean, D., K. Huppi, M. Bell, L. Staudt, W. Gerhard, and M. Weigert. 1984. Generation of antibody diversity in the immune response of BALB/c mice to influenza virus hemagglutinin. *Proc. Natl. Acad. Sci. USA* 81: 3180–3184.
- Zhang, J., I. C. MacLennan, Y. J. Liu, and P. J. Lane. 1988. Is rapid proliferation in B centroblasts linked to somatic mutation in memory B cell clones? *Immunol. Lett.* 18: 297–299.
- Allen, C. D., T. Okada, H. L. Tang, and J. G. Cyster. 2007. Imaging of germinal center selection events during affinity maturation. *Science* 315: 528–531.
- Blink, E. J., A. Light, A. Kallies, S. L. Nutt, P. D. Hodgkin, and D. M. Tarlinton. 2005. Early appearance of germinal center-derived memory B cells and plasma cells in blood after primary immunization. *J. Exp. Med.* 201: 545–554.
- Dörner, T., H. P. Brezinschek, R. I. Brezinschek, S. J. Foster, R. Domiati-Saad, and P. E. Lipsky. 1997. Analysis of the frequency and pattern of somatic mutations within nonproductively rearranged human variable heavy chain genes. *J. Immunol.* 158: 2779–2789.
- Longo, N. S., P. L. Lugar, S. Yavuz, W. Zhang, P. H. Krijger, D. E. Russ, D. D. Jima, S. S. Dave, A. C. Grammer, and P. E. Lipsky. 2009. Analysis of somatic hypermutation in X-linked hyper-IgM syndrome shows specific deficiencies in mutational targeting. *Blood* 113: 3706–3715.
- Liu, Y. J., and J. Banachereau. 1997. Regulation of B-cell commitment to plasma cells or to memory B cells. *Semin. Immunol.* 9: 235–240.
- Lanzavecchia, A., N. Bernasconi, E. Traggiai, C. R. Ruprecht, D. Corti, and F. Sallusto. 2006. Understanding and making use of human memory B cells. *Immunol. Rev.* 211: 303–309.
- Luckey, C. J., D. Bhattacharya, A. W. Goldrath, I. L. Weissman, C. Benoist, and D. Mathis. 2006. Memory T and memory B cells share a transcriptional program of self-renewal with long-term hematopoietic stem cells. *Proc. Natl. Acad. Sci. USA* 103: 3304–3309.
- Schmidlin, H., S. A. Diehl, and B. Blom. 2009. New insights into the regulation of human B-cell differentiation. *Trends Immunol.* 30: 277–285.
- Ozaki, K., R. Spolski, R. Ettinger, H. P. Kim, G. Wang, C. F. Qi, P. Hwu, D. J. Shaffer, S. Akilesh, D. C. Roopenian, et al. 2004. Regulation of B cell differentiation and plasma cell generation by IL-21, a novel inducer of Blimp-1 and Bcl-6. *J. Immunol.* 173: 5361–5371.
- Ettinger, R., G. P. Sims, A. M. Fairhurst, R. Robbins, Y. S. da Silva, R. Spolski, W. J. Leonard, and P. E. Lipsky. 2005. IL-21 induces differentiation of human naive and memory B cells into antibody-secreting plasma cells. *J. Immunol.* 175: 7867–7879.
- Bryant, V. L., C. S. Ma, D. T. Avery, Y. Li, K. L. Good, L. M. Corcoran, R. de Waal Malefyt, and S. G. Tangye. 2007. Cytokine-mediated regulation of human B cell differentiation into Ig-secreting cells: predominant role of IL-21 produced by CXCR5+ T follicular helper cells. *J. Immunol.* 179: 8180–8190.
- Thoree, V. C., S. J. Golby, L. Boursier, M. Hackett, D. K. Dunn-Walters, J. D. Sanderson, and J. Spencer. 2002. Related IgA1 and IgG producing cells in blood and diseased mucosa in ulcerative colitis. *Gut* 51: 44–50.
- Yavuz, S., A. C. Grammer, A. S. Yavuz, T. Nanki, and P. E. Lipsky. 2001. Comparative characteristics of mu chain and alpha chain transcripts expressed by individual tonsil plasma cells. *Mol. Immunol.* 38: 19–34.

Corrections

Frölich, D., C. Giesecke, H. E. Mei, K. Reiter, C. Daridon, P. E. Lipsky, and T. Dörner. 2010. Secondary immunization generates clonally related antigen-specific plasma cells and memory B cells. *J. Immunol.* 185: 3103–3110.

In Fig. 1, the dot plot shown at day 5 was incorrectly shown as a duplication of the dot plot shown at day 6. The corrected Fig. 1 is reprinted below. The figure legend was correct as published and is shown below for reference.

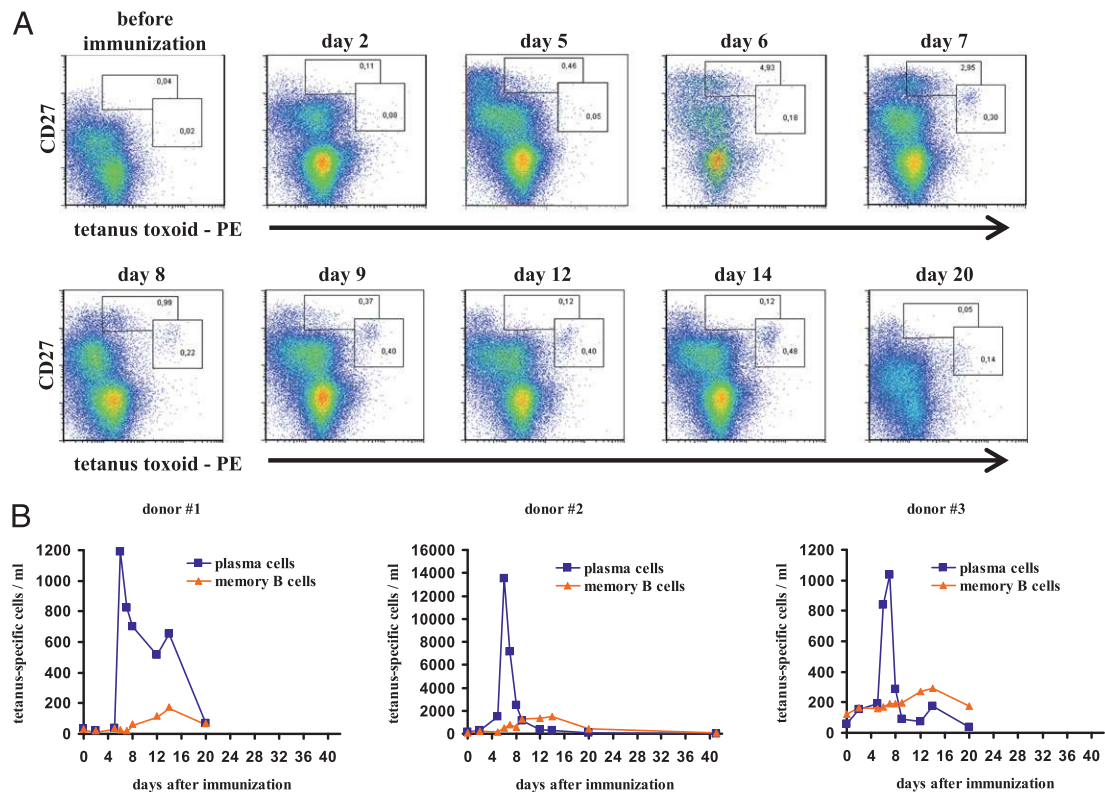


FIGURE 1. Kinetics of TT-specific PCs and memory B cells in peripheral blood. *A*, Dot plots of cytometric analysis of PE-labeled TT-specific CD19⁺, CD27⁺⁺, CD3⁻, CD14⁻ PCs and CD19⁺, CD27⁺, CD3⁻, CD14⁻ memory B cells of donor #2. *B*, Time course of appearance of PCs and memory B cells for each donor. Blue diamonds and orange squares indicate time points of blood analyses.

www.jimmunol.org/cgi/doi/10.4049/jimmunol.1390063